Hindawi
Discrete Dynamics in Nature and Society
Volume 2023, Article ID 8520036, 7 pages
https://doi.org/10.1155/2023/8520036

Research Article

Components' Tolerance Impact on the Design of a Real Case of One MW PV Substation

Ramzi Ben Ayed,[1] Rawia Chakroun ,[1] Nabil Derbel ,[1] and Abdellatif Ben Makhlouf [2]

[1]*Control & Energy Management Laboratory (CEMLab), Digital Research Center of Sfax (CRNS), University of Sfax, Sfax Engineering School, BP 1173, Sfax 3038, Tunisia*
[2]*Department of Mathematics, College of Science, Jouf University, Sakaka, Aljouf, Saudi Arabia*

Correspondence should be addressed to Abdellatif Ben Makhlouf; abmakhlouf@ju.edu.sa

Received 24 October 2022; Revised 16 November 2022; Accepted 2 January 2023; Published 19 January 2023

Academic Editor: Juan L. G. Guirao

In this article, a real case of a one MW PV substation design problem is described. The impact of the tolerances of power components (mainly inductors and capacitors) on the design is highlighted through two studies using two different control strategies that are selective harmonic elimination (SHE) and selective harmonic modulation (SHM). The obtained results show that the components' tolerances have a significant effect on the design, especially for the SHE strategy. While the design using SHM control shows a weak sensitivity to the components' tolerance. In this study, an upgrade of the most sensitive control strategy is proposed in order to improve its sensitivity against components' tolerance. The results show that the strategy upgrading leads not only to improving the sensitivity but also to generating better power quality.

1. Introduction

Today, PV systems are widely used with other green energies in order to reduce the environmental impacts, especially global warming. However, the use of strong PV stations has a significant influence on the quality of electrical energy generated due to harmonics rejected on the distribution grid. Three key standards and regulations that are IEEE 519 [1], G5/4 [2], and French Decree 2008 [3], are recommended as grid codes to minimize the rejected harmonics.

To be aligned with these grid codes, a lot of works based on Patel and Hoft [4] are proposed. From these works, it is clear that an LCL [5] and an LLCL filter [6] combined with a selective harmonic elimination (SHE) [4] and a selective harmonic modulation (SHM) shall be used. In [7], a real case of a one MW PV is proposed, and a comparison of generated energy quality with LCL and LLCL combined with the SHM and SHE strategy [8] is shown, but until now, there is no research that demonstrates the effect of the suggested tolerance on the design of the PV system. Based on prior research, this work aims to investigate the influence of the PV system's component tolerances. Furthermore, a lot of design methodologies such as [9] propose an innovative solution for solving and optimizing design problems. For control design strategies combined with filter design among the famous research studies by Patel and Hoft since 1973 [4] and Franquelo et al. [5], it is demonstrated that, for such design problem, SHM design strategy allows to fit the rejected current spectrum under the allowed gauge imposed by standards. However, in this article, it is demonstrated that an upgraded SHE strategy leads to better results. The effort spent to upgrade this control strategy is not important, thanks to mathematical algorithm solvers and powerful calculators. Besides, this effort is compensated by a better power quality generated on the grid.

The structure of this article is as follows. The problem description of a one MW PV system with an LLCL filter is shown in Section 2 [10]. In Section 3, a brief presentation of SHE and SHM strategies is made. The impact of components' tolerance is analysed through the results obtained from SHE and SHM strategies combined with the LLCL filter obtained in Section 4. In Section 5, a radical solution is

proposed to secure the design and make it totally independent from components' tolerances. Section 6 is devoted to the conclusion.

2. Problem Description of a Real Case of One MW PV Substation

Figure 1 depicts the proposed PV system's topology.

Figure 2 depicts the analogous circuit for each phase.

The per-phase equivalent frequency diagram after the ignorance of the resistance in front of the inductance impedance is depicted in Figure 3.

This system is already presented in [11]. The filter inductor is integrated with the transformer to lower the overall volume and weight of the system, resulting in cost savings. The tertiary inductor is caused by the leakage inductance of the cables used to link the capacitor's bank to the tertiary: it is also proved in [11] that this parameter has a significant influence on harmonic rejections.

3. SHE and SHM Theories

SHE and SHM theories are described in the following sections.

3.1. SHE Control Strategy. The selective harmonic elimination suggested by Patel and Hoft consists of solving mathematical equations where all of them must be equal to zero in order to find the position of n switching angles.

Considering k is the number of switching angles, n is the harmonic order, and angles $\alpha_i\,(i = 1, \ldots, k)$, the following equations were generated, where $T\,\mathrm{mod}_n$ is the harmonic amplitude of n^{th} order which is expressed by

$$T\,\mathrm{mod}_n = \frac{4}{n\pi}\left|1 + 2\sum_{i=1}^{k}(-1)^i \cos n\alpha_i\right|, \tag{1}$$

for $n = 5, 7, 11, \ldots, q$.

Theoretical investigation of the problem aims to zero out a large number of unique odd harmonics using the SHE method [12]. The factors are listed as follows to make up a valid SHE solution:

$$0 < \alpha_1 < \ldots < \alpha_i < \alpha_{i+1} < \ldots < \alpha_n < \frac{\pi}{2}, \tag{2}$$

where each α_i is the switching angle at which the inverter must alter the output voltage, with $i = 1, \ldots, n$. This indicates that, in order to eliminate n harmonics with $n = 5, 7, 11, \ldots, q$, a solution α_i must fulfill the following set of equations, which are provided in the following equations:

$$M_d = T\,\mathrm{mod}_1 = \frac{4}{\pi}\left|1 + 2\sum_{i=1}^{k}(-1)^i \cos\alpha_i\right|. \tag{3}$$

The required modulation index is M_d:

$$0 = \frac{4}{n\pi}\left|1 + 2\sum_{i=1}^{k}(-1)^i \cos n\alpha_i\right|, \tag{4}$$

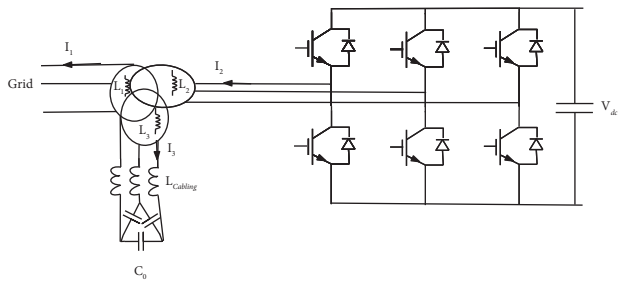

Figure 1: General power system topology.

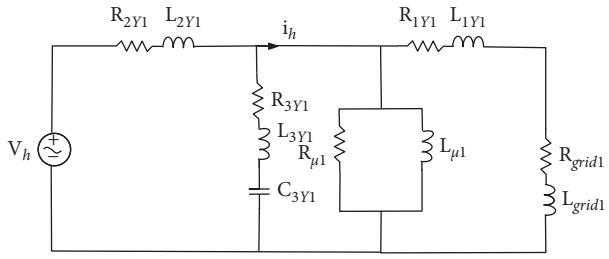

Figure 2: Equivalent circuit for each phase.

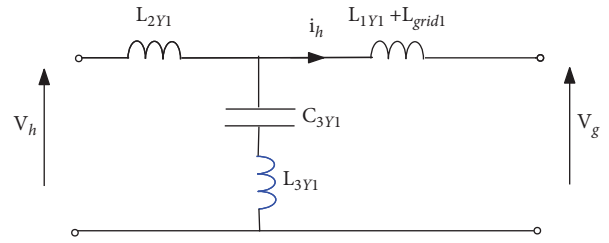

Figure 3: Frequency diagram modeling for each phase.

where $n = 5, 7, 11, \ldots, q$, and a good solution must adhere to the restrictions of equation (2).

3.2. SHM Control Strategy. The selective harmonic modulation consists of solving the same mathematical equations developed by Patel and Hoft but here n inequalities shown should be solved as follows:

$$\mathrm{OF} = \left(T\,\mathrm{mod}_1 - M_d\right)^2. \tag{5}$$

Depending on equation (2), as well as

$$\begin{aligned} T\,\mathrm{mod}_5 &\le L_5, \\ T\,\mathrm{mod}_7 &\le L_7, \\ T\,\mathrm{mod}_q &\le L_q, \end{aligned} \tag{6}$$

where M_d denotes the requested modulation index, L_5, L_7, and $L_{11}, \ldots, L_q$ are the limits which are calculated to guarantee that grid codes should be respected.

4. Tolerances Impact on the Design

4.1. Sequential Quadratic Programming. Optimization of electrical system design [13] is currently a commonly utilized practical method [14]. The SHE [15] and SHM inequalities

may be solved using a variety of strategies [16] as a consequence of developments in computer science and numerical concept [17]. We suggest applying optimization techniques, especially a deterministic approach [18], to reduce the size and complexity of the optimization issue [19]. Many algorithms have been studied [20], but the well-known Sequential Quadratic Programming (SQP) algorithm has ultimately been chosen as the current approach for handling challenging nonlinear and restricted programming issues [21].

4.2. Desired Modulation Index M_d. Yearly worldwide irradiation surpasses 2 kwh/m^2, the PV substation is meant to run in southern Tunisia. It is assumed that the PV station will normally run in around its nominal mode. The desired nominal value is 0.86.

4.3. Applicable Tolerances. A lot of datasheets from different capacitors and inductors suppliers have been analysed. Almost, a $(-10\%, +10\%)$ tolerance is considered on inductors. However, a bigger tolerance shall be considered on the leakage inductor L_{3Y1} introduced by cables. Indeed, a lot of the parameters are involved in the calculation of this leakage inductance that themselves are dependent on the tolerance:

(i) A tolerance on cable length

(ii) A tolerance on the measuring equipment using in the test bank to estimate the linear leakage inductance of the tertiary cable

(iii) A tolerance on the leakage inductance of the transformer tertiary

Considering all of these arguments, a tolerance of at least 30% should be taken into account for L_{3Y1}.

4.4. Impact on the Transfer Function of the System. Considering the respective tolerances on each component of the PV system shown in Figure 3, the lower response of the transfer function, given in Section 1, can be easily deduced as per the following equation:

$$F_{\text{Min}} = \frac{1 + p^2 N_1}{p\left(L_1' + p^2 D_1\right)}, \tag{7}$$

where $p = j\omega$, and N_1, L_1', and D_1 are defined as

$$\begin{aligned} N_1 &= C_{3Y1\min} L_{3Y1\min}, \\ L_1' &= L_{1Y1\min} + L_{2Y1\min} + L_{\text{grid1}}, \\ G_1 &= C_{3Y1\min}\left(L_{2Y1\min} + L_{3Y1\min}\right)\left(L_{1Y1\min} + L_{\text{grid1}}\right), \\ D_1 &= G_1 + L_{2Y1\min} L_{3Y1\min} C_{3Y1\min}. \end{aligned} \tag{8}$$

The upper response of the transfer function can be easily deduced as per the following equation:

$$F_{\text{Max}} = \frac{1 + p^2 N_2}{p\left(L_2' + p^2 D_2\right)}, \tag{9}$$

where N_2, L_2', and D_2 are defined as

$$\begin{aligned} N_2 &= C_{3Y1\max} L_{3Y1\max}, \\ L_2' &= L_{1Y1\max} + L_{2Y1\max} + L_{\text{grid1}}, \\ G_2 &= C_{3Y1\max}\left(L_{2Y1\max} + L_{3Y1\max}\right)\left(L_{1Y1\max} + L_{\text{grid1}}\right), \\ D_2 &= G_2 + L_{2Y1\max} L_{3Y1\max} C_{3Y1\max}. \end{aligned} \tag{10}$$

The responses of transfer functions F_{Min} and F_{Max} are shown in Figure 4 as well as the initial value considered in the initial study.

The F_{Min} response function shows a lower resonance and antiresonance frequencies than the initial transfer response than a better filter attenuation behavior at high frequency, especially for the higher harmonics orders.

The F_{Max} response function shows a higher resonance and antiresonance frequencies than the initial transfer function responses, which leads to the worst attenuation behavior of the filter at high frequencies, especially from the 23$^{\text{rd}}$ harmonic order. Thus, there is a big risk to break grid codes to confirm this risk, the voltage spectrum obtained by SHM and SHE is injected on both F_{Min} and F_{Max} transfer functions, and the current spectrums are compared with grid codes.

Figure 5 shows both harmonic current spectrums obtained by SHM and SHE with F_{Min} and F_{Max}. Indeed, by adopting the SHM method, the 23$^{\text{rd}}$ harmonic is more concerned with grid standards than the influence of component tolerances on PV design.

So to conclude, grid codes are respected when the SHM strategy is chosen regardless of the components' tolerances but when SHE is chosen, components' tolerances have a big impact on the current spectrum tolerances. So the risk to break grid codes is too high.

However, with the SHM strategy even if the grid code is respected, nonzero low-frequency current harmonics are seen and will lead to a high value of THD contrary to the harmonic current spectrum obtained by SHE where low-frequency current harmonics are eliminated except the 23$^{\text{rd}}$ harmonic that breaks grid codes. For this reason, a radical solution is proposed in the next section in order to mitigate the risk to break grid codes and to avoid the negative impact of component's tolerances on the design when SHE is used.

5. Tolerances' Impact on the Design

In the previous section, the advantage of SHE is highlighted. However, with SHE the risk to break grid codes is very high because the tolerances of the PV system could impact the transfer function of the system and move the resonance and antiresonance over a frequency range where the upper and the lower value are related to the upper and lower value of components' tolerances. In the studied case, the 23$^{\text{rd}}$ harmonic exceeds the limit of the grid codes where SHE seven switching angles are used.

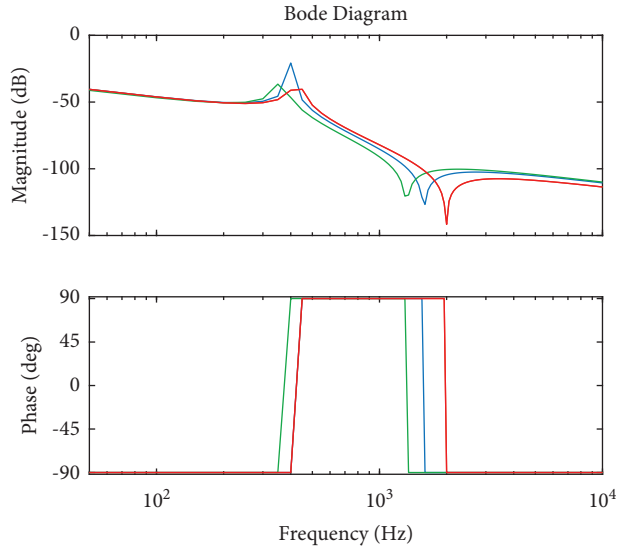

Figure 4: Bode plot of initial values (in blue), F_{Min} (in red), and F_{Max} (in green).

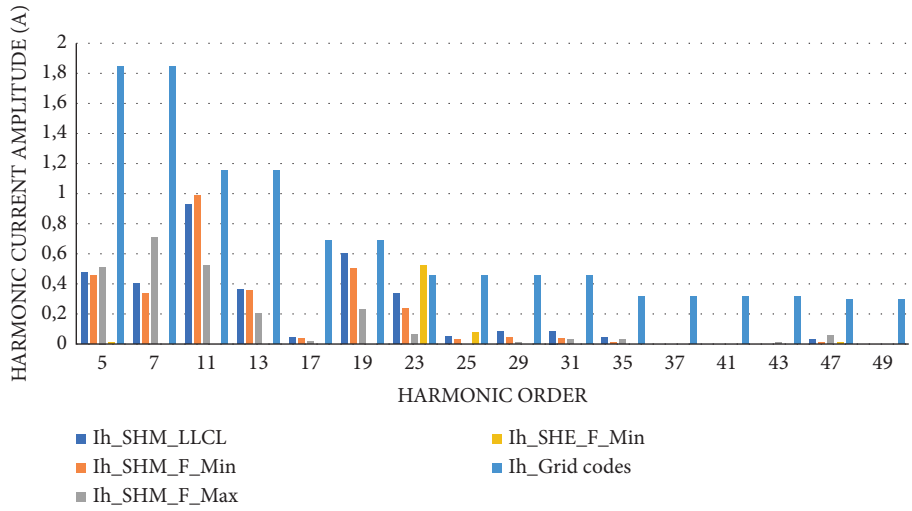

Figure 5: Harmonic current spectrums obtained by SHM and SHE versus grid codes.

5.1. Proposed Method for Theoretical Analysis. In order to handle this problem, the proposed solution consists of increasing switching angles to eight in order to eliminate the 23rd harmonics and let the filter eliminate the higher current harmonics orders that remain totally uncontrolled. The eight switching angles strategy could be expressed in an (OF) subject to

$$T \bmod_5 \le c_5, \tag{11}$$

$$T \bmod_7 \le c_7, \tag{12}$$

$$T \bmod_{11} \le c_{11}, \tag{13}$$

$$T \bmod_{13} \le c_{13}, \tag{14}$$

$$T \bmod_{17} \le c_{17}, \tag{15}$$

$$T \bmod_{19} \le c_{19}, \tag{16}$$

$$T \bmod_{23} \le c_{23}, \tag{17}$$

$$0 < \alpha_1 < \alpha_2 < \alpha_3 < \alpha_4 < \alpha_5 < \alpha_6 < \alpha_7 < \alpha_8 < \frac{\pi}{2}, \tag{18}$$

where all constraints are given from equations (11)–(18).

$c_5, c_7, c_{11}, c_{13}, c_{17}, c_{19}$, and c_{23}, are approximated to 0. The obtained current harmonic spectrum is shown and compared to grid codes in Figure 6.

Figure 6 shows that the first seven harmonics are deleted and that the grid codes are followed. Both SHM with seven switching angles and SHE with eight switching angles respect grid codes, but the SHE eight switching angles are more consuming than SHM, but this is justified by the better THD.

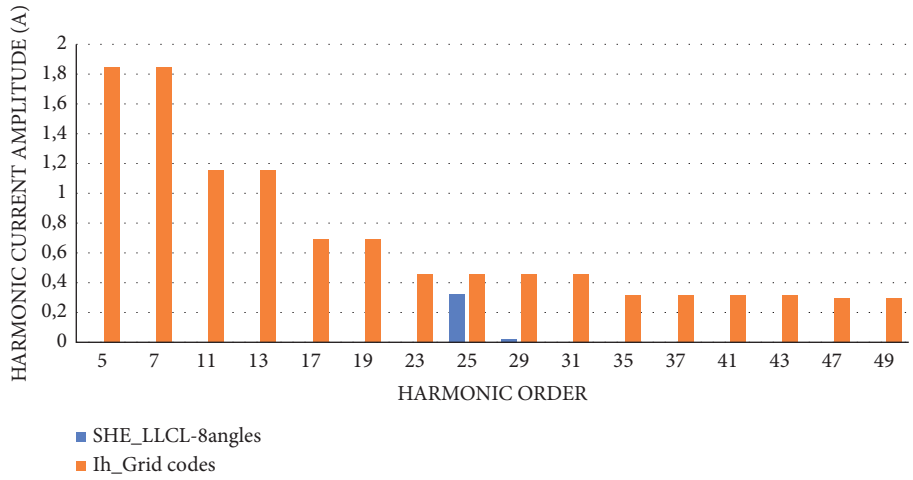

Figure 6: Harmonic current spectrum of SHE-LLCL with eight switching angles.

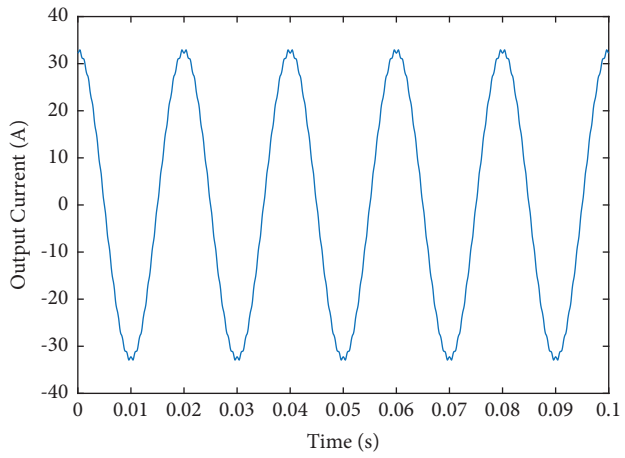

Figure 7: Obtained output current of the proposed solution (eight switching angles).

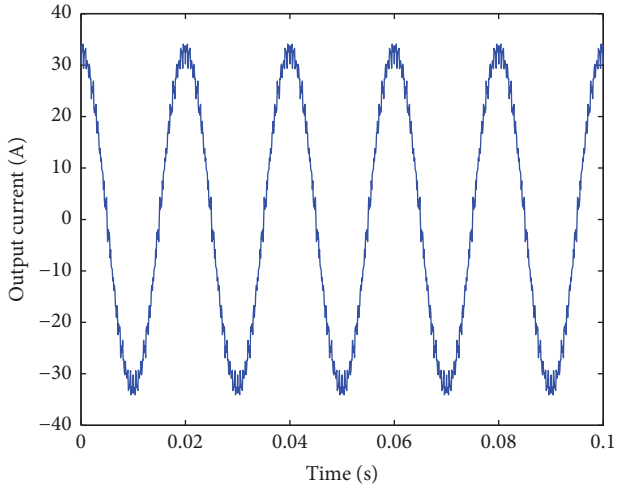

Figure 8: Obtained output current of the adopted SHM-LLCL strategy.

5.2. Time-Domain Comparison. The output current curve generated using the combined SHE-LLCL with eight switching angles is shown in Figure 7. With this approach, the THD [22] is 1.4%.

Figure 8 depicts the current injected into the grid using the SHM-LLCL approach. This technique yielded a THD of 5.92%.

Both curves produce good results because THD is less than 8% (the most prevalent THD accepted on power networks globally). The combined SHE-LLCL approach with eight switching angles outperforms the SHM-LLCL technique in terms of THD. Indeed, using the SHM method, persistent low-frequency harmonics produce an increase in THD. However, in the suggested method, SHE-PWM eliminates low-frequency harmonics that are damaging to the network, and the optimized LLCL filter attenuates the 23rd harmonic, which explains the given findings. This result reinforces the suggested solution's efficiency in terms of offering greater power quality and performance [23]. The motivation behind moving away from traditional studies persists not only by its high amplitude attenuation of all harmonics regarding grid codes standards but also by its capability of handling several problems that may occur by avoiding the unwanted effect of SHE-PWM taking into account the impact of component's tolerances. Indeed, the proposed methodology is an efficient strategy, which is based on deterministic optimization, compared to previous works adopted in literature in terms of performance and providing high-quality power.

6. Conclusion

This article shows the components' tolerance drawback on the design of a one MW PV substation. The comparison of both control strategies that are SHE and SHM considering inductors and capacitors' tolerances shows that, with the SHM strategy, grid code is respected but with a high THD level. However, with the SHE strategy, the components' tolerances could lead to break grid codes and this should be anticipated during the design phase by upgrading the SHE strategy in order to remove harmonics from resonance and

antiresonance zones. The upgrading of SHE will lead to a much more complicated mathematical problem to solve, but this is easy to mitigate thanks to the optimization algorithm. The proposed research methodology not only complies with grid regulations but also provides a lower THD value and higher quality of generated energy on the grid. The positive point of this work is the real aspect of the photovoltaic power station, which could match with all distribution worldwide. Therefore, it could be considered as a real solar project and a better alternative to be realized in the future.

Symbols

R_{2Y1}: Secondary winding resistance (Ω)
L_{2Y1}: Secondary inductance (H)
$L_{2Y1\min}$: Minimum secondary inductance value (H)
$L_{2Y1\max}$: Maximum secondary inductance value (H)
R_{3Y1}: Tertiary resistance (Ω)
L_{3Y1}: Tertiary inductance (H)
$L_{3Y1\min}$: Minimum tertiary inductance value (H)
$L_{3Y1\max}$: Maximum tertiary inductance value (H)
C_{3Y1}: Tertiary capacitance (H)
$C_{3Y1\min}$: Minimum tertiary capacitance value (H)
$C_{3Y1\max}$: Maximum tertiary capacitance value (H)
R_{1Y1}: Primary winding resistance (Ω)
L_{1Y1}: Primary inductance (H)
$L_{1Y1\min}$: Minimum primary inductance (H)
$L_{1Y1\max}$: Maximum primary inductance (H)
$R_{\mu 1}$: Magnetic resistance (Ω)
$L_{\mu 1}$: Magnetic inductance (H)
R_{grid1}: Equivalent grid resistance (Ω)
L_{grid1}: Equivalent grid inductance (H).

Data Availability

The data used to support the study are included within the article.

Conflicts of Interest

The authors declare that they have no conflicts of interest.

References

[1] IEEE, "IEEE Recommended Practice and Requirements for Harmonic Control in Electric Power Systems," 2014, https://ieeexplore.ieee.org/servlet/opac?punumber=6826457.

[2] Energy networks association, *Engineering Recommendation G5/4, Recommendation Planning Levels for Harmonic Voltage Distortion and the Connection of Non-linear-equipement to Transmission Systems and Distribution Networks in the United Kingdom*, Energy Networks Association, London, UK, 2001.

[3] République française, *Relatif aux prescriptions techniques de conception et de fonctionnement pour le raccordement à un réseau public de distribution d'électricité en basse tension*, République française, France, Europe, 2011.

[4] H. S. Patel and R. G. Hoft, "Generalized techniques of harmonic elimination and voltage control in thyristor inverters: Part I–Harmonic Elimination," *IEEE Transactions on Industry Applications*, vol. 3, pp. 310–317, 1973.

[5] L. G. Franquelo, J. Napoles, R. C. P. Guisado, J. I. Leon, M. A. Aguirre, and M. A. Aguirre, "A flexible selective harmonic mitigation technique to meet grid codes in three-level PWM converters," *IEEE Transactions on Industrial Electronics*, vol. 54, no. 6, pp. 3022–3029, 2007.

[6] J. Napoles, J. I. Leon, R. Portillo, L. G. Franquelo, and M. A. Aguirre, "Selective harmonic mitigation technique for high-power converters," *IEEE Transactions on Industrial Electronics*, vol. 57, no. 7, pp. 2315–2323, 2010.

[7] W. Wu, Y. He, and F. Blaabjerg, "An LLCL power filter for single-phase grid-tied inverter," *IEEE Transactions on Power Electronics*, vol. 27, no. 2, pp. 782–789, 2012.

[8] R. Chakroun, R. Ben Ayed, and N. Derbel, "Comparison between LCL and LLCL filters for a grid connected inverter using selective harmonic modulation," in *Proceedings of the 2020 5th International Conference on Renewable Energies for Developing Countries (REDEC)*, pp. 1–6, IEEE, Marrakech, Morocco, June 2020.

[9] F. F. Juárez Regalado, D. Esenarro, M. Diaz Reátegui, and M. Frayssinet Delgado, "Model based on balanced scorecard applied to the strategic plan of a peruvian public entity," *3c Empresa: Investigacion Y Pensamiento Crítico*, vol. 10, no. 4, pp. 127–147, 2021.

[10] K. Arulkumar, D. Vijayakumar, and K. Palanisamy, "Design of optimal LLCL filter with an improved control strategy for single phase grid connected PV inverter," *International Journal of Power Electronics and Drive Systems*, vol. 9, no. 1, pp. 114–125, 2018.

[11] R. Chakroun, R. B. Ayed, and N. Derbel, "Combined SHE-LLCL design for a real case photovoltaic power station," *Journal of Control, Automation and Electrical Systems*, vol. 31, no. 6, pp. 1558–1566, 2020.

[12] P. L. Kamani and M. A. Mulla, "Online she technique for cascaded multilevel inverters with adjustable dc sources," *International Journal of Power and Energy Systems*, vol. 40, no. 4, 2020.

[13] K. Shi, J. Wang, S. Zhong, Y. Tang, and J. Cheng, "Non-fragile memory filtering of TS fuzzy delayed neural networks based on switched fuzzy sampled-data control," *Fuzzy Sets and Systems*, vol. 394, pp. 40–64, 2020.

[14] K. Shi, J. Wang, Y. Tang, and S. Zhong, "Reliable asynchronous sampled-data filtering of T-S fuzzy uncertain delayed neural networks with stochastic switched topologies," *Fuzzy Sets and Systems*, vol. 381, pp. 1–25, 2020.

[15] S. Kundu, D. B. Arka, S. K. Giri, S. Mukherjee, and S. Banerjee, "Implementation of selective harmonic minimization PWM on seven-level cascaded h-bridge inverter with improved inverter performances and equal power sharing among cells," in *Proceedings of the 2017 International Conference on Power and Embedded Drive Control (ICPEDC)*, pp. 348–353, IEEE, Chennai, India, March 2017.

[16] X. Cai, S. Zhong, J. Wang, and K. Shi, "Robust H^{∞} control for uncertain delayed TS fuzzy systems with stochastic packet dropouts," *Applied Mathematics and Computation*, vol. 385, Article ID 125432, 2020.

[17] S. Hu, H. Huang, and D. Czarkowski, "Hybrid trigonometric differential evolution for optimizing harmonic distribution," in *Proceedings of the 2005 IEEE International Symposium on Circuits and Systems (ISCAS)*, pp. 1306–1309, IEEE, Kobe, Japan, May 2005.

[18] M.-H. Lin, J.-F. Tsai, and C. S. Yu, "A review of deterministic optimization methods in engineering and management," *Mathematical Problems in Engineering*, vol. 2012, pp. 1–15, 2012.

[19] S. Hu, H. Huang, and D. Czarkowski, "Fuzzy solution for approximating constrained optimal PWM using quantum evolutionary algorithm," in *Soft Methodology and Random Information Systems*, pp. 661–668, Springer, Berlin, Heidelberg, 2004.

[20] A. K. Singh Yadav, M. Sora, and M. Sora, "An optimized deep neural network-based financial statement fraud detection in text mining," *3c Empresa: Investigacion Y Pensamiento Critico*, vol. 10, no. 4, pp. 77–105, 2021.

[21] R. Chakroun, R. Ben Ayed, and N. Derbel, "A Comparative analysis between SQP and PSO for optimizing a one MW PV substation,"vol. 1, pp. 1–6, in *Proceedings of the 2022 5th International Conference on Power Electronics and their Applications (ICPEA)*, vol. 1, IEEE, Hail, Saudi Arabia, March 2022.

[22] S. Debnath and R. N. Ray, "THD optimization in 13 level photovoltaic inverter using genetic algorithm," *International Journal of Engineering Research in Africa*, vol. 2, no. 3, pp. 385–389, 2012.

[23] N. Maqache and A. J. Swart, "Remotely measuring and controlling specific parameters of a PV module via an RF link," *3C Tecnología_Glosas de innovación aplicadas a la pyme*, vol. 10, no. 4, pp. 103–129, 2021.